AIChE

A Quantitative Proteomic Analysis of Cellular Responses to High Glucose Media in Chinese Hamster Ovary Cells

Zhenke Liu, Shujia Dai, Jonathan Bones, Somak Ray, Sangwon Cha, and Barry L. Karger
Barnett Inst. and Dept. of Chemistry and Chemical Biology, Northeastern University, Boston, MA 02115

Jingyi Jessica Li
Dept. of Statistics, University of California, Los Angeles, CA 90095

Lee Wilson, Greg Hinckle, and Anthony Rossomando
Alnylam Pharmaceuticals, Cambridge, MA 02142

DOI 10.1002/btpr.2090
Published online 00 Month 2015 in Wiley Online Library (wileyonlinelibrary.com)

A goal in recombinant protein production using Chinese hamster ovary (CHO) cells is to achieve both high specific productivity and high cell density. Addition of glucose to the culture media is necessary to maintain both cell growth and viability. We varied the glucose concentration in the media from 5 to 16 g/L and found that although specific productivity of CHO-DG44 cells increased with the glucose level, the integrated viable cell density decreased. To examine the biological basis of these results, we conducted a discovery proteomic study of CHO-DG44 cells grown under batch conditions in normal (5 g/L) or high (15 g/L) glucose over 3, 6, and 9 days. Approximately 5,000 proteins were confidently identified against an mRNA-based CHO-DG44 specific proteome database, with 2,800 proteins quantified with at least two peptides. A self-organizing map algorithm was used to deconvolute temporal expression profiles of quantitated proteins. Functional analysis of altered proteins suggested that differences in growth between the two glucose levels resulted from changes in crosstalk between glucose metabolism, recombinant protein expression, and cell death, providing an overall picture of the responses to high glucose environment. The high glucose environment may enhance recombinant dihydrofolate reductase in CHO cells by up-regulating NCK1 and down-regulating PRKRA, and may lower integrated viable cell density by activating mitochondrial- and endoplasmic reticulum-mediated cell death pathways by up-regulating HtrA2 and calpains. These proteins are suggested as potential targets for bioengineering to enhance recombinant protein production. © 2015 American Institute of Chemical Engineers *Biotechnol. Prog.*, 000:000–000, 2015
Keywords: proteomics, Chinese hamster ovary cells, high glucose, recombinant protein expression, bioprocessing, glucose metabolism, biotherapeutics, cell death, 2DLC, MS

Introduction

Chinese hamster ovary (CHO) cells are the most widely used production cell line for the manufacture of recombinant human biotherapeutic proteins because of their ability toexhibit proper protein folding and human-like post-translational modifications, in particular glycosylation.[1] CHO cell production processes currently can reach titers in the grams per liter range, more than a 100-fold increase over titers of the mid-1980s.[2] However, many studies have reported that very high specific productivities, i.e., productivity of recombinant protein per cell,[3] are accompanied with slowly growing cell lines.[4–10] A goal in recombinant protein production is to achieve high specific productivity with enhanced cell density of viable cells and culture longevity.[11] It is, therefore, important to understand the reasons for the slow cell growth while the specific productivity is high. One way, this can be accomplished is by an in-depth examination of the biological processes (BPs) involved by proteomic analysis.

The process of recombinant protein synthesis results in a significant cellular energy demand, and further increases in the specific productivity of protein production raise this energy requirement further.[12] Glucose is widely used as a key energy source in serum-free chemically defined media; however, with high levels of glucose, toxic metabolites from

Current address of Zhenke Liu and Anthony Rossomando: Synageva BioPharm, 33 Hayden Ave., Lexington, MA 02421

Current address of Shujia Dai: Sanofi Oncology Discovery and Preclinical Sciences, 640 Memorial Drive, Cambridge, MA 02139

Current address of Jonathan Bones: NIBRT—the National Inst. for Bioprocessing Research and Training, Fosters Ave., Mount Merrion, Blackrock, Co., Dublin, Ireland

Current address of Sangwon Cha: Dept. of Chemistry, Hankuk University of Foreign Studies, Yongin, 449791, South Korea

Additional Supporting Information may be found in the online version of this article.

Correspondence concerning this article should be addressed to B. L. Karger at b.karger@neu.edu

glucose metabolism can be generated at levels that are detrimental to cell growth and protein synthesis.[13] Abnormally high levels of glucose can induce a series of specific cellular responses. For example, increases in lactate production,[13] reactive oxygen species (ROS),[14,15] endoplasmic reticulum (ER) stress,[16] apoptosis,[14,15] necrosis,[17] and protein synthesis[18] have been observed. Furthermore, CHO cells cultured under normal or high glucose conditions behave as two very different phenotypes in terms not only of glucose metabolism, but also of the level of recombinant protein synthesis and cell death.[18] However, because of the potential of nonenzymatic glycation of recombinant protein products,[19] high glucose media is generally not recommended for the cultivation of industrial cell lines. Nevertheless, high glucose concentration, in comparison with normal levels, can be a useful model to explore key pathways that manipulate protein production and cell growth.

A number of proteomic studies have been published that explore the biology of CHO cell lines used for production of therapeutic proteins[5,6,20–28] (reviewed in Ref. [29]). These studies have revealed many pathways that are involved in diverse biological functions related to recombinant protein production. To conduct such studies, the need exists for a CHO cell proteome database with functional annotation. The genomic sequence of several CHO cell lines, including CHO-K1, DG44, and CHO-S[30,31] and protein sequence databases[32,33] of the CHO-K1 strain have recently become available. Here, we used an mRNA expression-based database for CHO DG44 that was annotated to mouse homologues.

In this study, by culturing CHO-DG44 cells expressing anti-CD20 monoclonal antibody (mAb) in media with 5, 8, 12, and 16 g/L glucose in batch mode, we observed decreased integrated viable cell density (IVCD), increased cell death, and higher specific productivity with increased glucose concentration. To examine further the molecular basis of these culture results, proteomic profiles of CHO-DG44 cells, expressing an empty vector containing the recombinant dihydrofolate reductase (rDHFR) gene cultured in 15 g/L glucose, were quantitatively compared with the normal level of 5 g/L glucose-containing media across different cell-growth stages (exponential, stationary, and death), as shown in Figure 1. Proteomic analysis resulted in the identification of almost 5,000 nonredundant proteins, of which 2,800 were quantified with at least two peptides. A self-organizing map (SOM) algorithm was utilized for clustering and deconvolution of the temporal profiles of differentially regulated proteins when comparing the two concentration levels of glucose. Key regulatory proteins involved in crosstalk between glucose metabolism, antioxidant response, recombinant protein expression, and cell death were observed. These findings provide novel insight and potential protein targets, such as NCK1, PRKRA, high temperature requirement A 2 (HtrA2), and calpains, for cell engineering to enhance simultaneously specific productivity of recombinant protein and cell growth in CHO cells.

Materials and Methods

Materials

Formic acid, triethylammonium bicarbonate (TEAB), dithiothreitol, iodoacetamide, and ammonia were purchased from Sigma (St. Louis, MO). Sequence-grade modified trypsin was obtained from Promega (Madison, WI), and the bicinchoninic acid (BCA) protein assay kit was from Pierce (Rockford, IL). RapiGest™ SF surfactant was from Waters Corporation (Milford, MA). Liquid chromatography-mass spectroscopy (LC-MS) grade water was purchased from J. T. Baker (Phillipsburg, NJ), and LC-MS grade acetonitrile was from VWR (West Chester, PA). The tandem mass tag (TMT) 6-plex kit was obtained from Thermo Fisher Scientific (Rockford, IL).

CHO-DG44 cell culture

CHO-DG44 cells were purchased from Life Technologies (A11000-01) and grown in 250-mL shake flasks (Corning, Tewksbury, MA) containing 50 mL of serum-free culture medium (Gibco CD DG44 Medium) with L-glutamine and Pluronic F-68 and incubated in a Multitron II orbital shaker (ATR, Laurel, MD) set at 37 °C and 5% CO_2. Cultures were grown under batch conditions (no additional feeding following Day 0), seeded at 5×10^5 cells/mL with different concentrations of glucose added to the medium. Cell cultures used for proteomics analysis were cultured in media containing 5 or 15 g/L glucose and harvested on Day 3, 6, and 9. Five milliliters of each sample was then centrifuged at 1,000 rpm to pellet the cells, with the pellet stored at −80 °C until needed. Prior to conducting this study, CHO-DG44 cells were stably transfected with a previously reported[34] plasmid vector containing an anti-CD20 mAb gene sequence (bioreactor studies) or an empty plasmid vector without no transgene expressed (proteomic studies) containing the DHFR gene controlled by a cytomegalovirus promoter. Viable cell densities (VCDs) were measured using a Multisizer Coulter Counter (Beckman Coulter, Fullerton, CA). Lactate dehydrogenase (LDH) assay was performed using a CytoTox 96V R non-radio cytotoxicity LDH Assay (Promega) according to the manufacturer's recommendation. The amount of harvested anti-CD20 mAb was quantified using a Bradford assay kit (Bio-Rad Laboratories, Hercules, CA) with a previously purified and quantified (ultraviolet absorbance at 280 nm) anti-CD20 mAb as a standard.

Cell lysis, protein digestion, and peptide labeling

A pellet consisting of approximately 5,000,000 cells was reconstituted in 0.1% w/v RapiGest in 500 mM TEAB and heated at 95 °C for 5 min. After cooling on ice, the reconstituted pellet was sonicated for 90 s in an ice-bath (1 s sonication and 4 s rest, 30 s sonication per cycle, three cycles in total). Next, the homogenized solution was centrifuged at 16,000*g* for 10 min, and the supernatant was aspirated. The protein concentration in the supernatant was determined using the BCA protein assay, with the lysis buffer being used to eliminate any background absorbance from the RapiGest and TEAB. The extracted protein solution was then reduced with a final concentration of 5 mM dithiothreitol at 60 °C for 30 min and alkylated with a final concentration of 15 mM of iodoacetamide in the dark at room temperature for 30 min. Tryptic digestion was performed overnight with the enzyme to protein ratio of 1:40 (w/w) at 37 °C.

Protein digests (100 μg per TMT channel) from cell cultures of four cell growth time points (Days 0, 3, 6, and 9) in high or normal glucose media were labeled with 4 TMT channels (127, 128, 129, and 130, respectively) from the TMT 6-plex kit (Table 1), according to the manufacturer's instructions. A globally pooled peptide mixture from all the

Table 1. TMT Labeling

	127	128	129	130	131
High glucose (HG)	Day 0 (*H*)	Day 3 (*H*)	Day 6 (*H*)	Day 9 (*H*)	Replicate*
Normal glucose (NG)	Day 0 (*N*)	Day 3 (*N*)	Day 6 (*N*)	Day 9 (*N*)	Replicate*

Replicate*: pooled sample of all eight samples.

eight samples (two glucose concentrations, each with four time points) was labeled with one TMT channel (131) as replicates in all experiments. All five TMT channels were mixed together in equal amounts based upon the starting protein concentration (BCA assay). The mixture was acidified using trifluoroacetic acid to pH < 2 and incubated for 45 min at 37 °C to promote hydrolysis of the Rapigest. The hydrolyzed Rapigest was next precipitated by centrifugation at 14,000*g* for 10 min, and the supernatant was carefully aspirated and stored at −80 °C prior to LC-MS analysis.

2D LC-MS/MS

About 200 μg of labeled and pooled protein digest was analyzed by two-dimensional high pH/low pH reversed phase/reversed phase (RP/RP) LC[35] coupled to a hybrid LTQ Orbitrap XL mass spectrometer (Thermo Fisher Scientific). The pooled protein digest was initially fractionated by high pH RPLC using a narrow bore Gemini C18 column (15 cm × 1.0 mm i.d., 5 μm particle size, 110 Å pore size; Phenomenex, Torrance, CA). The platform consisted of an Ultimate LC pump (Dionex, Thermo Fisher Scientific), an Agilent 1200 series diode array detector (Agilent Technologies, Santa Clara, CA) and a Gilson FC 203B fraction collector (Middleton, WI). Mobile phases A and B were 20 mM ammonium formate in water, pH 10, and 20 mM ammonium formate in 90% acetonitrile/10% water, respectively. A three-step linear gradient was used for the separation at 150 μL/min (4% B to 10% B in 2 min, 10% B to 45% B in 33 min, and 45% B to 100% B in 2 min). Twenty eight fractions were collected in 90-s intervals across the LC gradient. Based on the UV (214 nm) intensity profile, fractions were merged to 22 comparable peptide level fractions for analysis in the second-dimension low-pH LC-MS analysis. Each fraction was centrifuged to dryness under vacuum and stored at −80 °C until analysis.

For the second dimension nanoLC-MS analysis, each aliquot was reconstituted in 7 μL of 0.1% formic acid in water, and 5 μL was injected. The low-pH RPLC platform was composed of an Ultimate 3000 LC pump (Dionex) and a self-packed C18 column (20 cm × 75 μm ID column, 5 μm 300 Å Vydac C18 particles; Grace Davison Discovery Sciences, Deerfield, IL). Mobile phases C and D were 0.1% formic acid in water and 0.1% formic acid in acetonitrile, respectively. A four-step linear gradient was used for the separation (2% D to 6% D in 2 min, 6% D to 24% D in 240 min, 24% D to 40% D in 18 min, and 40% D to 80% D in 2 min). The flow rate was maintained at 300 nL/min during loading and desalting and then reduced to 200 nL/min for the separation.

MS data were collected in data-dependent mode, with a survey MS scan, followed by five collision-induced dissociation (CID) and five higher-energy collisional dissociation (HCD) MS/MS scans for the five most intense precursor ions. Full MS scans were acquired in the Orbitrap, with a resolution of 15,000 at *m*/*z* 400. CID spectra were obtained in the LTQ with normalized collision energy of 35%. HCD spectra were acquired in the Orbitrap with resolution 7,500 at *m*/*z* 400, an isolation window of 1.5 Da, an automatic gain control target of 5E4, with a maximum ion injection time 500 ms and normalized collision energy of 48%.

Construction and annotation of CHO-DG44 cell proteome database

CHO-DG44 transcriptome sequences were pooled from published transcriptome data[36] and in-house sequencing data by Roche 454 (Branford, CT) using 50-base, single-end runs. The final transcriptome data were assembled using CLC Genomics Workbench Version 4 (http://www.clcbio.com/) with the NCBI mouse RefSeq set of transcripts (http://www.ncbi.nlm.nih.gov/refseq/) as reference. For annotating the resulting CHO transcript, the same mouse sequences that led to the creation of the CHO read in the CLC Genomics software were used. The RNA transcripts were translated to protein sequences using ESTScan version 3.0,[37] to predict protein coding regions from nucleotide sequences. For ESTScan unassigned transcripts, the translated longest open reading frame was considered as the protein sequence.[38]

Protein identification and quantitation

Raw files were processed by Proteome Discoverer version 1.3 (Thermo Fisher Scientific). MS/MS spectra were searched using Mascot 2.3 against the in-house curated CHO-DG44 database. Cysteine carbamidomethylation (+57 Da) and 6-plex TMT (+299 Da) modification at the *N*-terminal and ε-amino residues on the side chain of lysines were set as fixed modifications. Up to two missed cleavages were allowed for tryptic digestion. Both HCD and CID MS/MS spectra were combined and used for peptide identification. Mass tolerances were set at 10 ppm for the precursor ions, 0.8 Da for the fragment ions in the CID-MS^2 spectra, and 0.05 Da for the fragment ions in the HCD-MS^2 spectra. A MASCOT ion score of ≥ 20 was used as criterion for each peptide. The false discovery rate (FDR) in peptide identification was controlled to below 1% by Proteome Discoverer 1.3 using a decoy database.[39] Only proteins containing unique peptides were considered.

Relative peptide quantitation was performed using Proteome Discoverer 1.3. Briefly, the peak intensities of TMT reporter ions in HCD-MS^2 spectra were extracted and integrated with 10 mmu mass tolerance using the "centroid sum" mode. The isotope correction matrix for 6-plex TMT was used. Relative peptide abundances were determined by the ratios of peak intensities of the reporter ions, with channels 128, 129, and 130 representing samples from Day 3, 6, and 9, respectively, relative to the samples from Day 0 (channel 127). The protein ratio was estimated from the median of the "unique peptide spectral match" ratios for the given protein. In the case where an even number of the unique peptide spectral match ratios existed, the geometric mean of the two middle ratios was calculated by Proteome Discoverer. Experimental bias correction based on the

Table 2. Calculation of Expression Ratio of High Glucose/Normal Glucose Over Time Course

Day 3	Day 6	Day 9	Replicate
$\frac{\text{Day 3 } (H)/\text{Day 0 } (H)}{\text{Day 3 } (N)/\text{Day 0 } (N)}$	$\frac{\text{Day 6 } (H)/\text{Day 0 } (H)}{\text{Day 6 } (N)/\text{Day 0 } (N)}$	$\frac{\text{Day 9 } (H)/\text{Day 0 } (H)}{\text{Day 9 } (N)/\text{Day 0 } (N)}$	$\frac{\text{Replicate/Day 0 } (H)}{\text{Replicate/Day 0 } (N)}$

protein median was also active, and the median protein ratio was normalized to 1.

Through the procedures described earlier, we calculated the ratio of 128/127, 129/127, 130/127, and 131/127 in each glucose concentration, representing the protein expression ratio of Day 3, 6, and 9, respectively, to Day 0 and the corresponding replicate. We thus obtained protein temporal profiles within each glucose concentration. Here, we considered the Day 0 time point, the inoculum, as the beginning of cell culture (before the addition of any glucose). As both cultures were prepared from this single inoculum, cells on Day 0 are biologically identical between the two conditions.

For a protein at each time point, we obtained a protein expression ratio $R(H) = \text{Day } x(H)/\text{Day } 0(H)$ in high glucose concentration and $R(N) = \text{Day } x(N)/\text{Day } 0(N)$ in normal glucose concentration. Because cells on Day 0 are biologically identical between the two conditions, we calculated $R(H)/R(N)$ to obtain the differential expression of this protein between high and normal glucose concentrations on Day x (Table 2).

The temporal trend across the three time points of protein expression ratios between the two glucose concentrations were clustered based on the SOMs algorithm. Proteins with significantly up- or down- regulation trends between two glucose concentrations were proposed as the functionally associated proteins.

Self-organizing maps

The two technical replicate ratios for common proteins were pooled. The total number of common proteins falling within a range of variations (namely, 10%, 20%, 30%, etc.) from the population mean, 1, was calculated.[40]

The temporal profiles of quantified protein expression ratios between two glucose concentrations were then submitted to the GenePattern platform[41] for further cluster analysis. An unsupervised learning approach, SOM,[42,43] was utilized to deconvolute the temporal profiles of protein expression patterns across the three cell-growth phases (3, 6, and 9 days). To generate reproducible clustering results, the major parameters for SOM algorithm were set according to the recommended parameters by the SOMClustering algorithm (version 2).[44] The number of clusters was set at five, and seed for the random number generator was set at 42. Random vectors were used to select initial random centroids. Alpha initial and final values were set at 0.1 and 0.005, respectively, and sigma initial and final values were set at 5.0 and 0.5, respectively. The top two clusters generated by SOM, representing statistically significantly up- or down- regulated proteins between the CHO cell cultures (high vs. normal glucose conditions) over the three cell growth phases, were selected for biological function analysis.

Gene ontology enrichment and ingenuity pathway analysis

Biological analysis was performed using Database for Annotation, Visualization, and Integrated Discovery (DAVID; http://david.abcc.ncifcrf.gov/tools.jsp)[45,46] and Ingenuity Pathway Analysis (IPA, Ingenuity® Systems, Redwood City, CA, http://www.ingenuity.com). In DAVID, the function of quantitated CHO cell proteins were analyzed based on the corresponding mouse homologue RefSeq annotation. Gene ontology (GO)[47] terms and KEGG pathways (http://www.kegg.jp/) in DAVID were visualized using an Enrichment Map[48] plug-in in Cytoscape[49] with suggested parameters. In IPA, experimental data from human, mouse, and rat were used for analysis of protein pathways and networks. A P-value of 0.05 was selected as the significant threshold for pathway analysis in IPA.

Results

Characterization of cell culture responses

Initial investigations focused on the characterization of the cellular responses to the high glucose environment by monitoring IVCD, LDH activity in cell culture supernatants, and specific productivity (Figure 2). We batch cultured in duplicate CHO-DG44 cells expressing anti-CD20 mAb in media with 5, 8, 12, and 16 g/L glucose. When the glucose concentration increased from 5 to 16 g/L, IVCD decreased by 46% (Figure 2A) and LDH activity in cell culture supernatant, a measure of cell death, increased (Figure 2B), whereas specific productivity increased by 56% (Figure 2C). As expected, increased glucose levels in the media induced not only lower levels of IVCD from higher levels of the cell death, but at the same time, higher levels of recombinant protein synthesis per cell in the CHO-DG44 cell line. Efforts were made to ensure reproducibility in cell cultures, including cell growth curves, viability of cells, and other parameters, to achieve a biologically repeatable process of each phenotype in a well-controlled bench-top scale. The standard error of the mean (Supporting Information Table S1) for each data point is included as y-error bars (Figure 2), indicating good biological reproducibility.

Cell cultures for LC-MS analysis

To elucidate the general cellular response differences (i.e., independent of the specific recombinant protein product) between normal and high glucose concentrations, we used CHO-DG44 cell line only expressing DHFR[50] on a plasmid vector devoid of any transgene as a model system. It has been shown that cell lines expressing only rDHFR often exhibit different cellular behaviors compared with their counterparts expressing mAb in addition to rDHFR.[51] Cell lines expressing different biologics could exhibit different cellular behaviors. However, the pathways with glucose susceptibility are expected to be similar in both conditions. Therefore, cells with an empty expression vector were used to eliminate the high background attributable to the recombinant protein while allowing relevant measurements of cell productivity. Also, because this project was the initial investigation, we used batch culture, which is the basic mode of cell culture and is easy to control. Although it is different from other used culture modes, the pathways responding to high glucose elucidated here should provide hypotheses to be tested in other modes.

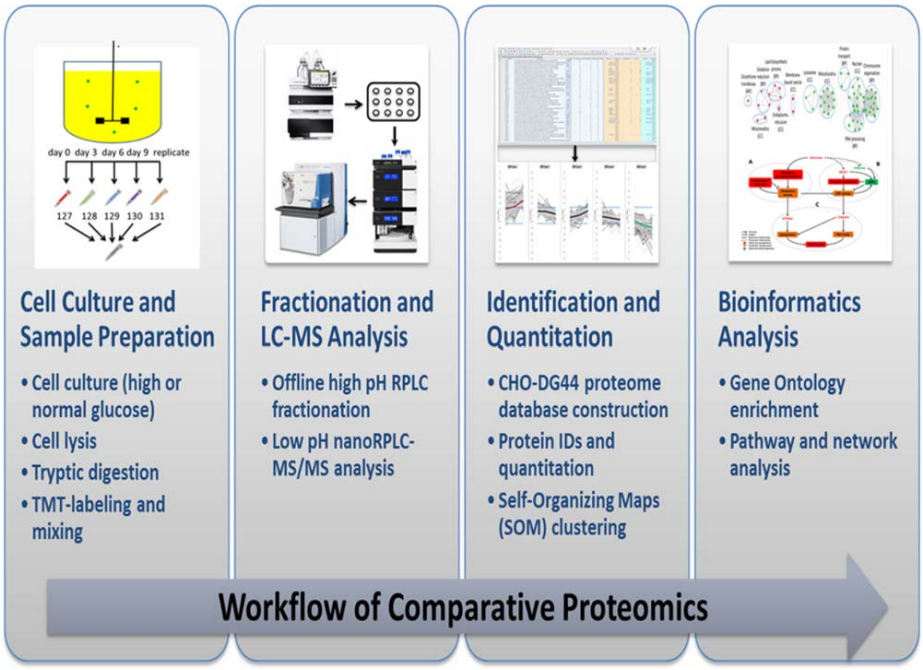

Figure 1. Workflow of comparative proteomics.

For simplicity, a glucose concentration of 5 g/L was chosen as the normal level because it has been widely used for CHO cell culture in biopharmaceutical industry and 15 g/L as the higher level, according to the above experimental results of cell culture.

The cell growth responses during the batch mode cell culture to the two glucose media concentrations were examined by monitoring IVCD and VCD, as shown in Figure 3. Similar to the results in Figure 2A, IVCD of the cell culture decreased in high glucose media, relative to normal glucose media (Figure 3A). In addition, the high glucose culture had a reduced VCD (Figure 3B), indicating that a higher glucose level led to lower cell growth, in agreement with what was found previously.[18] A good reproducibility of cell culture parameters, such as IVCD and VCD, between batches was observed, as depicted in Figure 3 by the very narrow error bars (see associated numbers in Supporting Information Table S2), again indicating the key cell culture conditions were well controlled between biological replicates.

Cells from four time points, Days 0, 3, 6, and 9, were analyzed by comparative proteomics (Figure 1). The use of the high-resolution 2D-RP/RPLC-MS platform allowed high coverage of the CHO cell proteome. CID and HCD spectra from the LTQ Orbitrap XL were combined to increase peptide identification, and HCD spectra were used for reporter ion quantitation. To reduce potential interference for reporter ions, a narrow isolation window of 1.5 *m/z* was selected.[52,53]

Protein identification and quantitation

The constructed CHO-DG44 database contains 16,357 protein entries, annotated from mouse RefSeq sequences. Based on more than 34,700 unique peptides with 1% FDR,[39] 4,986 nonredundant proteins were identified, with 3,910 proteins overlapping between the two experiments. (Only proteins that were quantified at all four time points were included.) Proteins detected in only one condition could represent genes with all-or-none expression and, thus, play significant roles in determining the cell physiology under different conditions. However, the limited detection could result from an insufficient sampling capability of the data-dependent proteomics method. To obtain an accurate ratio for the following analyses, only proteins detected in both conditions were included. Statistical and biological analyses were performed for 2,800 proteins quantified with at least two peptides in both the high and normal glucose samples.

A commonly selected threshold for significant change, 1.2 fold,[54–58] was chosen in this work. To estimate the technical variation of the TMT-based quantitative method, a globally pooled mixture from all samples was labeled with TMT-131 and mixed equally (based on mass) with the other TMT-labeled samples for Days 0, 3, 6, and 9. As shown in Supporting Information Figure S1, more than 92% of the protein ratios derived from technical replicates showed less than 20% variance from the nominal ratio (1:1), in agreement with what has been reported by others,[40] suggesting overall good technical reproducibility.

Self-organizing map clustering

As described earlier, the relative protein expression levels were normalized to the Day 0 time point. The temporal expression profiles of protein ratios from high vs. normal glucose levels were clustered using the SOM algorithm.[42] The SOM is a clustering algorithm with unsupervised learning that converts complex, nonlinear statistical relationships between high-dimensional data sets into simple geometric relationships with a nonlinear low-dimensional display,[42,43] i.e., protein expression patterns. The SOM clustering algorithm used for downstream analysis allows us to track expression trends of proteins that showed significant changes for two glucose treatments across the three time points over the duration of the batch culture. This trend analysis relies on sampling at multiple time points after treatment in

contrast to sampling replicates at the same point in time, which is commonly used for differential expression analysis. Additionally, the temporal approach used herein requires that proteomic data generated across the time points be highly correlated with the cell growth parameters. The necessity for this high correlation further ensures confidence in the differential proteomics data and the associated inference of differential cell biology resulting from culture in media containing low or high concentrations of glucose.

We tested three to seven clusters for SOM. We found that five clusters represent a good compromise between the sensitivity (detection of differential proteins using above threshold) and specificity (less nondifferential proteins were involved into the list of up- or down-regulated protein clusters). When we used three clusters, we found many differential proteins (high sensitivity), but poor specificity (many nondifferential proteins were included). When we used seven clusters, we found that the differential proteins from top clusters are generally further classified based on the extent of fold-of-change, and that they are all significantly changed proteins, suggesting that further clustering is redundant. Five SOM clusters (Figure 4) indicate different protein responses across the cell culture lifespan (Days 3, 6, and 9). The protein ratios after SOM clustering showed the temporal expression patterns of the molecular responses. Proteins in SOM cluster 1, on average, increased in relative expression in high glucose media (up-regulated with time). In contrast, proteins in SOM cluster 5, on average, decreased (down-regulated with time). For proteins in SOM clusters 2, 3, and 4, most of the fold-changes fell within the 20% variance of the nominal ratio (1:1) and, thus, were considered not to be significantly changed. SOM clusters 1 and 5 consisted of 214 up- and 308 down- regulated proteins, respectively (Supporting Information Table S4).

Scatter plots of protein expressions between technical replicates or between samples in different days from 5 g/L and 15 g/L glucose media, as shown in Supporting Information Figure S2, demonstrated that expression changes of proteins in SOM clusters 1 and 5 resulted from different glucose concentrations in the media. In the scatter plot of replicate 1 vs. replicate 2, up-regulated proteins (red dots) and down-regulated proteins (green dots) are randomly overlapped due to the technical variation; however, in the scatter plots of 5 g/L vs. 15 g/L samples on Day 3, 6, and 9, the red and green dots are gradually separated into the >1.2 fold area and the <0.83 fold area, respectively. These observations agree with the up-regulated and down-regulated patterns of relative expression of proteins from cluster 1 or 5 across three stages, respectively, as shown in Figure 4.

The strict data analysis methods used in this article reduced potential over-statement of the results. One approach was the SOM clustering algorithm used for downstream analysis. Conventional differential proteomic studies contain two phenotypes, e.g., before and after treatment. Only one time point after treatment is generally selected and biologically repeated two or more times. The trend analysis used in this article relies on sampling at multiple time points, and only proteins showing robust changes across all three time points were selected. Additionally, the temporal approach used here requires that proteomic data generated across the time points be highly correlated with the cell growth parameters. This high correlation further ensures confidence in the differential proteomic data and associated inference of differential cell biology. The other approach was pathway analysis. All results presented in this article are based on the changes of multiple proteins in interacted pathway networks, rather than on the changes of random proteins. These two approaches increased the reliability of the results. The biological functions related to these proteins are discussed later.

Discussion

Gene ontology analysis

Proteins in clusters 1 and 5 were separately inputted into DAVID for functional enrichment analysis. The significantly enriched GO terms were filtered by FDR values less than 5% and visualized by a Cytoscape plug-in, Enrichment Map,[48] as shown in Figure 5. As discussed later, the GO terms in clusters 1 and 5 agree with the literature, supporting the clustering.

For the up-regulated proteins from SOM cluster 1, the enriched GO terms (Figure 5A) were classified into three categories: (1) BPs such as lipid biosynthesis and oxidation reduction; (2) cellular components such as mitochondria, ER, and membrane-bounded vehicle; and (3) molecular function such as glutathione transferase. BPs related to lipid synthesis, e.g., cholesterol biosynthesis and fatty acid metabolic processes, were found up-regulated in the CHO cells under the high glucose condition, relative to the normal concentration of glucose in the media. Such phenomena were also observed in renal proximal tubular cells[59] or macrophages.[60] Oxidation-reduction was up-regulated in CHO cells under the high glucose condition, likely because such a reaction is involved in glucose metabolism, lipid biosynthesis, and antioxidant response. Glutathione transferases, as the major antioxidant enzymes in glutathione-mediated detoxification of ROS, were found up-regulated under the high glucose condition. Such high glucose-induced up-regulation of the antioxidant response has been also reported in retinal pigmented epithelium cells.[61] In terms of localization, proteins in mitochondria, such as various NADH dehydrogenases and cytochrome C, were significantly enriched in the up-regulated protein cluster 1 in response to the high glucose stress, indicating their important roles in this subcellular organelle where oxidative phosphorylation and ROS generation occur.[62] Proteins in ER and Golgi (a membrane-bounded vehicle), such as 7-dehydrocholesterol reductase, 3-keto-steroid reductase, lathosterol oxidase, and fatty acid synthase, largely associated with the process of lipid synthesis,[63] were also up-regulated in protein cluster 1.

The enriched GO terms derived from down-regulated proteins in SOM cluster 5 (Figure 5B) were grouped into three BP clusters (chromosome organization, RNA processing, and protein transport) and three cellular component clusters (nuclear, mitochondria, and lysosome). CHO cells in the high glucose environment showed lower VCD, accompanied by down-regulated nuclear-associated processes such as chromosome organization, RNA processing, and protein transport, which have been previously associated with slower proliferation of cancer cells.[64,65] Furthermore, down-regulated mitochondrial proteins included many transporters such as voltage-dependent anion-selective channel proteins, mitochondrial import inner membrane translocase, and mitochondrial glutamate carrier 1, suggesting oxidative stress-induced mitochondrial dysfunction.[62] In addition, many lysosome enzymes involved in the breakdown of proteins and lipids were down-regulated, suggesting the down-regulation of lysosomal function in CHO cells under high glucose condition.

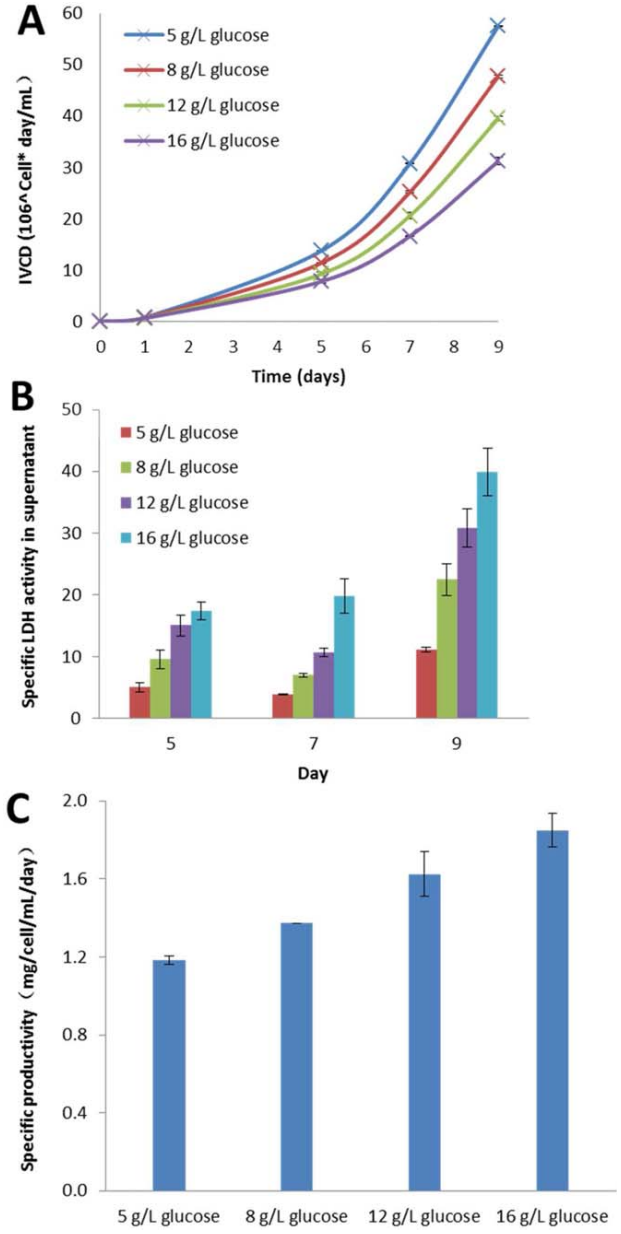

Figure 2. CHO-DG44 cell culture responses to increasing glucose concentration from 5 to 16 g/L in media.

A. Integrated viable cell density (IVCD) decreased. B. specific LDH activity (LDH activity/IVCD) in media supernatant increased. C. Specific productivity (protein production/IVCD) increased. Error bars represent ± SEM (standard error of the mean, $n = 2$).

The above enriched GO terms for up- and down-regulated proteins are tightly related to glucose metabolism, protein synthesis, and cell death. To understand how crosstalk could potentially impact cell growth and recombinant protein productivity inversely, we analyzed the key protein pathways and their downstream biological effects using IPA and DAVID.

Elevated oxidative phosphorylation and detoxification pathways in the high glucose condition

The 15 g/L concentration of glucose in the media, when compared with 5 g/L, seemed to enhance the expression of many proteins involved in oxidative phosphorylation and glutathione-mediated detoxification during cell culture (Figure 6A). The observed up-regulation of oxidative phosphorylation (Supporting Information Figure S3) indicates that, with the increase in media concentration, more glucose was oxidized in the aerobic respiration pathways, subsequently leading to an increased production of potentially harmful ROS by-products.[66,67] The up-regulation of the glutathione-mediated detoxification system (Supporting Information Figure S3) could be an adapted response to relieve the higher oxidative stress from the high glucose environment, although it is not expected to reverse the oxidative damage.[68]

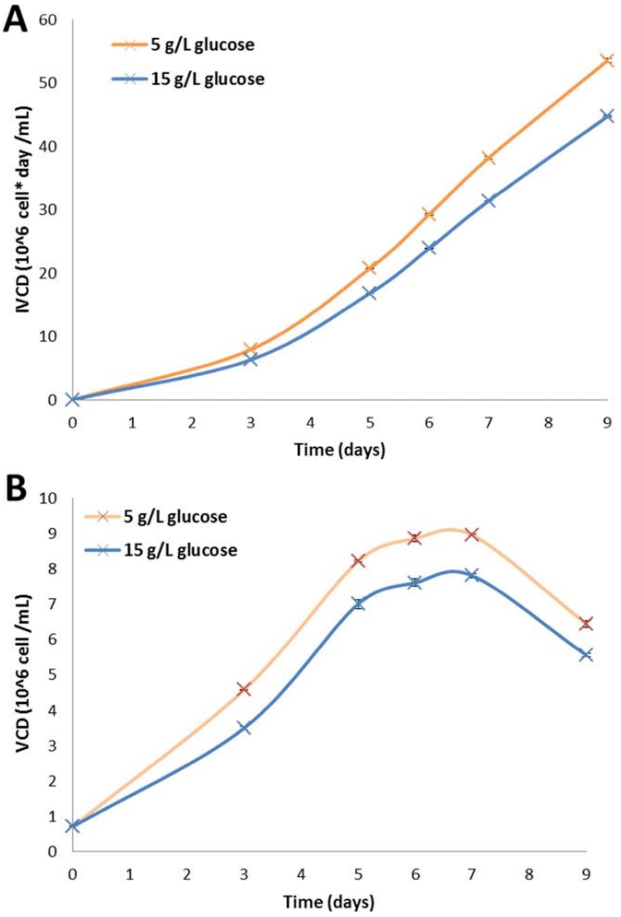

Figure 3. The integrated viable cell density (IVCD) (A) and viable cell density (VCD) (B) from biological replicates for batch mode cell cultures for both 5 and 15 g/L glucose media. Error bars represent ± SEM (standard error of the mean, $n = 2$).

Changes of rDHFR, NCK1, and PRKRA in the high glucose condition

It has been reported that high levels of ROS can induce ER stress, likely due to disturbed calcium homeostasis.[69] ER stress can activate a cellular stress response, the unfolded protein response (UPR), which decreases protein synthesis and activates protein degradation pathways.[70] Interestingly, CHO cells in high glucose media had a lower level of UPR. For the ubiquitin pathway, one of the major UPR pathways, five proteins were up-regulated, but nine were down-regulated (Supporting Information Figure S3), suggesting the down-regulation of protein degradation.

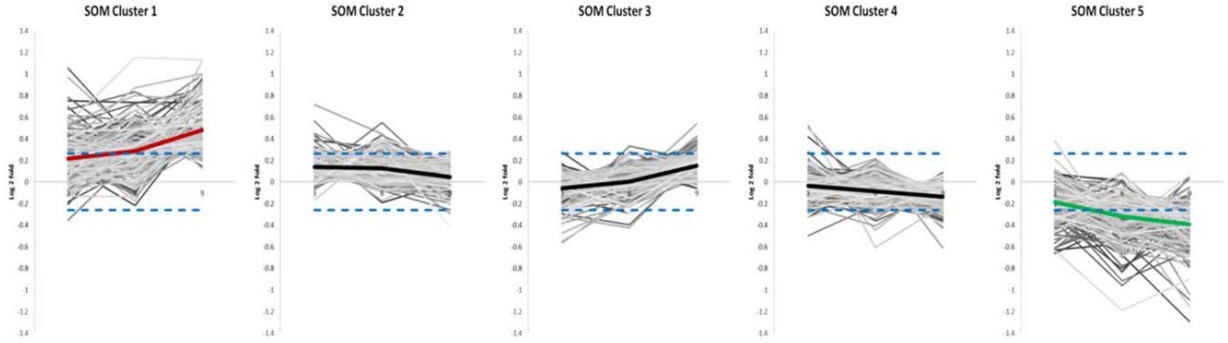

Figure 4. Five protein SOM clusters generated by GenePattern. The changes of 1.2-fold and 0.83-fold are highlighted by dotted lines.

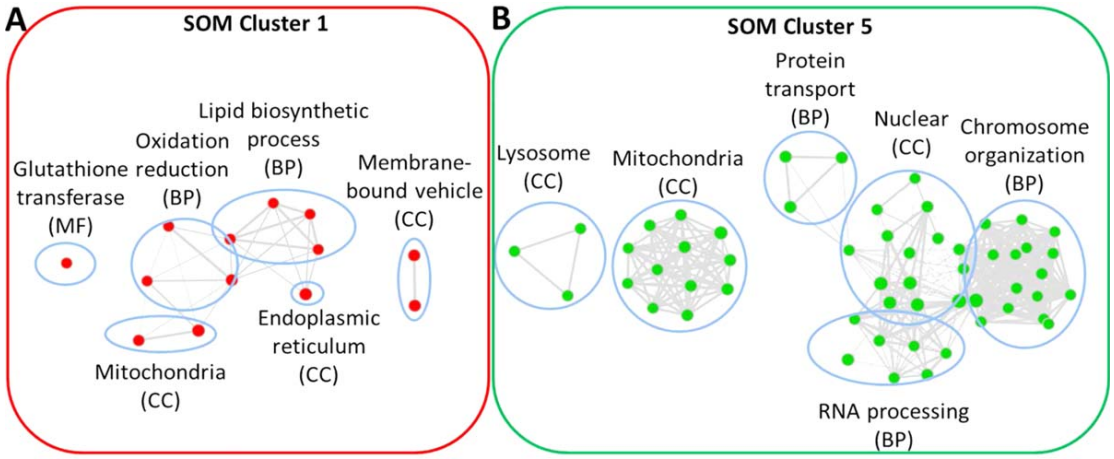

Figure 5. GO term enrichment in SOM clusters 1 (A) and 5 (B). BP: biological process; CC: cellular component; MF: molecular function.

The recombinant protein expressed in this CHO cell line, DHFR, was found in SOM cluster 1, and its levels were elevated in cells cultured in high glucose media as a function of cultivation time (Supporting Information Table S1). Usually, to facilitate the expression of the protein of interest in CHO-DG44 cells, the endogenous DHFR gene is deleted, and at the same time, the recombinant DHFR gene is incorporated into the expression vector. Because rDHFR is co-expressed with the gene of interest, the expression level of DHFR was used as an initial selection marker for high-production cell lines.[71] For the CHO-DG44 cell line used here, increased rDHFR expression in cells with the empty vector in high glucose media identified in proteomic study agreed with increased specific productivity levels in cells with IgG co-expressed (Figure 2).

Changes of other proteins involved in protein translation and folding also suggested enhanced recombinant protein expression with high glucose concentration. EIF2B2 (eukaryotic translation initiation factor 2B subunit 1 beta) was present in cluster 1, likely suggesting enhanced protein translation in high glucose cell culture. Furthermore, ER proteins involved in protein folding, e.g., FKBP7 (FK506-binding proteins 7), FKBP14, and calumenin, were up-regulated on all three days (in SOM cluster 1), likely suggesting up-regulated protein folding activity in the ER.

The up-regulation of NCK1 (noncatalytic region of tyrosine kinase adaptor protein 1) and down-regulation of PRKRA (protein kinase, interferon-inducible double stranded RNA dependent activator) in the high glucose cell culture were observed (Figure 6B). NCK1 is involved in signal transduction from receptor tyrosine kinases to downstream signaling pathways, regulating protein translation by modulating PERK (protein kinase RNA-like ER kinase), the latter of which inhibits translation initiation through phosphorylation of EIF2α (eukaryotic initiation factor 2α).[72,73] Overexpression of NCK1 has been demonstrated to inhibit transactivation of UPR related genes and to activate recombinant protein translation, thereby accelerating cell death under ER stress.[72,73] On the other hand, PRKRA (in SOM cluster 5) was highly down-regulated during the entire cell culture in the high glucose sample. The deactivation of PKR (protein kinase R) by PRKRA decreases UPR and recombinant protein expression.[74] High-production cell lines have been observed to be associated with inhibited UPR, but the detailed mechanism is not clear.[75] Our findings suggest that it may be due, in part, to up-regulation of NCK1 and PRKRA. In addition, because both proteins affect recombinant protein expression through the regulation of phosphorylation signaling,[72–74] phosphoproteomics could potentially be helpful to detail the associated signaling transduction pathways.

In summary, the up-regulation of NCK1 and down-regulation of PRKRA in the high glucose sample seem to contribute to the enhancement of rDHFR expression and likely compromised the activation of UPR for ER stress

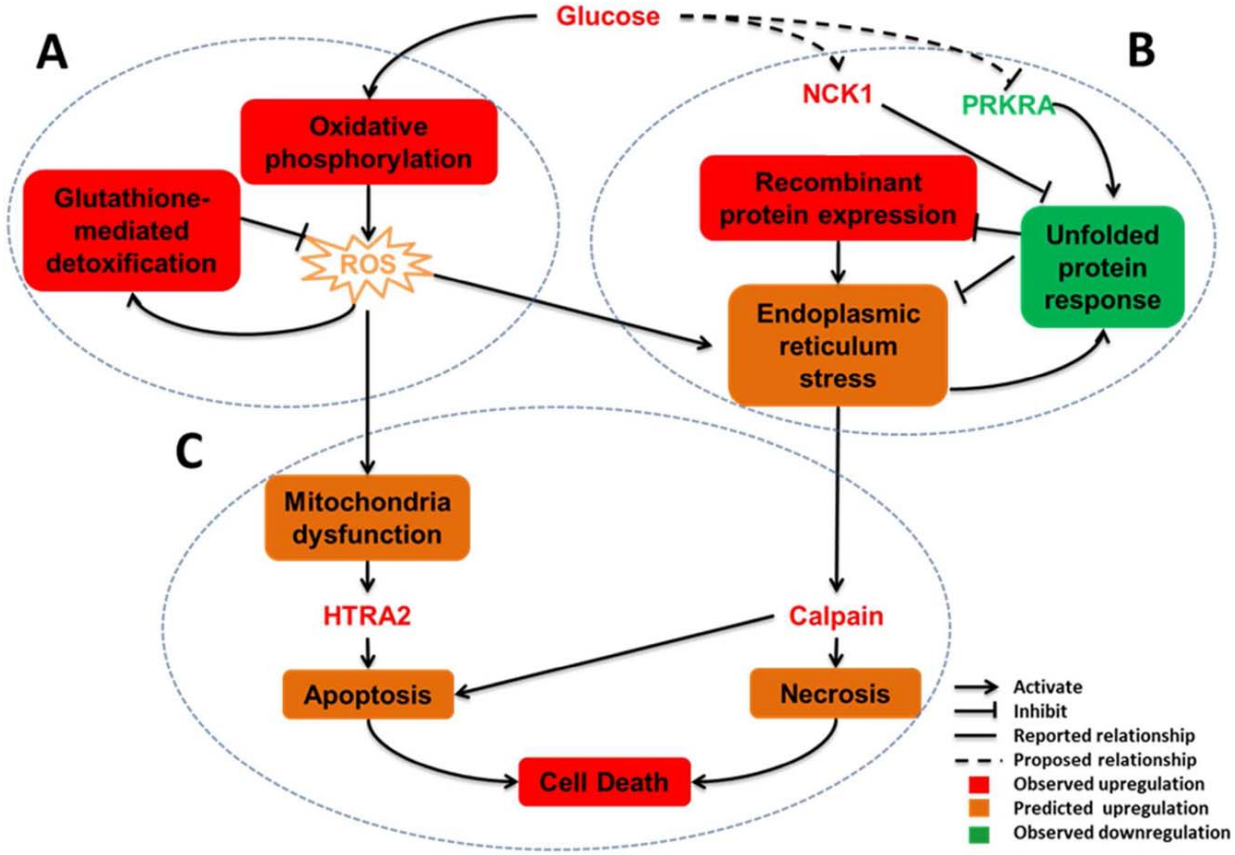

Figure 6. A simplified representation of interactions among glucose metabolism, recombinant protein expression, and cell death.

A. Glucose metabolism and antioxidant response. B. Recombinant protein expression. C. Cell death.

alleviation. ER stress as well as previously discussed oxidative stress could increase cell death.

Activated mitochondria- and ER-mediated cell death pathways

Analysis of the proteomic results suggested that the lower cell growth under the altered glucose metabolism induced by high glucose conditions likely resulted from higher cell death activated by mitochondria- and ER- mediated cell death pathways (Figure 6C). Up-regulated HtrA2 (in SOM cluster 1) correlated with high glucose induced cell death, suggesting the activation of mitochondria-mediated apoptosis in response to enhanced ROS production.[76–78] In agreement with this observation, the activators of cIAP, nuclear factor kappa-B (NFKB) 1 and 2 were down-regulated (in SOM cluster 5),[79] further contributing to apoptosis.

At the same time, up-regulated calpains (Capn1 and Capn5) were observed during high glucose induced cell death, suggesting that ER stress-mediated apoptosis and necrosis were also activated. Capn1 was up-regulated and its inhibitor, calpastatin,[80] down-regulated, both on Day 6. On the other hand, Capn5 (in SOM cluster 1) was up-regulated on all three days. The calpain family, a group of calcium-activated cysteine proteases, can enhance caspase-independent necrosis,[17,81] along with contributing to apoptosis.[69,82] In support of the above findings, high glucose has been reported to initiate necrosis by increasing the expression of Capn1, Capn2, and Capn10 (the analogue of Capn5 in a small subgroup) in pig kidney epithelial cells (LLC-PK1).[17] In addition, ROS H_2O_2 can cause necrosis of pancreatic acinar cells via increasing the expression of Capn1 and Capn2.[81] The function of Capn5 has not been well understood, except that the nematode orthologue of Capn5 has been known to facilitate necrotic cell death in *Caenorhabditis elegans*.[83]

Genetic engineering strategies to increase recombinant protein productivity

Throughout the proteomic study of CHO cells grown under normal and high glucose-containing media, several key regulators that control protein synthesis and cell death-related pathways were observed. Considering increased non-enzymatic glycation modifications on recombinant protein products under a higher concentration of glucose in the media,[19] we do not recommend achieving an optimized productivity by increasing glucose concentration in media. However, key proteins can be targeted as potential candidates for cell engineering not only to increase specific productivity but also to prevent cells from apoptosis or necrosis under the processes with normal glucose concentration. On the one hand, over-expression of NCK1 and knockdown of PRKRA (e.g., by small-interfering RNA, zinc finger proteins, etc.) could potentially lead to an enhanced specific productivity in CHO cells. On the other hand, HtrA2 and calpains (Capn1 and Capn5) can be potential knockdown targets to

inhibit cell death mediated by mitochondria dysfunction and ER stress, respectively, in CHO cell cultures.

In support of our results, engineering strategies targeting the above proteins have shown promising results in other cell lines. For example, over-expression of NCK1 has been demonstrated to increase recombinant protein expression in human embryonic kidney 293 (HEK293) cells and mouse embryonic fibroblast cells.[73] Down-regulation of PRKRA was found to enhance recombinant protein expression in HT1080 fibrosarcoma cells.[74] Silencing HtrA2 using siRNA reduces apoptosis induced by ultraviolet irradiation in U2OS cells (osteosarcoma cell line).[77] Inhibition of calpain 1 and 2 attenuates cell death induced by oxidative stress.[81] Therefore, manipulating these proteins could potentially improve recombinant protein productivity in CHO cells cultured even in normal conditions.

Currently, efforts in cell engineering to improve recombinant protein synthesis mainly focus on recombinant protein folding and secretion.[12] The manipulation of the protein translation machinery has been seldom reported, probably due to the complicated regulation and lack of potential individual protein/gene targets such as NCK1 or PRKRA shown here. Though reduction of cell death pathways has been a focused target of cell engineering, efforts have mainly centered on the death receptor- and mitochondrial-mediated apoptosis,[12] with one exception reporting the attempt to reduce ER-mediated apoptosis through down-regulation of ALG2 (alpha-1,3-mannosyltransferase).[84] In this study, beside the up-regulation of HtrA2 in mitochondrial-mediated apoptosis in CHO cells, our results suggest that cell death in CHO cells can also be influenced by ER stress through up-regulation of calpains, which can lead to caspase-independent necrosis.[17] This auxiliary cell death pathway needs to be also considered when anti-cell death strategies are attempted to reduce cell death using genetic engineering.

Conclusions

In this article, we have demonstrated the power of quantitative proteomics to elucidate the crosstalk among critical pathways in the process of CHO cell culture. Usually, CHO cell culture grown in high glucose containing media is not recommended for biopharmaceutical manufacturing due to the potential glycation modifications on recombinant proteins. However, the CHO cells grown in the above processes (normal or high glucose containing media) were utilized as a bioprocessing model for the study of pathway crosstalk among glucose metabolism, recombinant protein synthesis, and cell death. We have attempted to unveil the proteomic changes of CHO-DG44 cells in response to elevated glucose levels in media over the span of the cell culture. An annotated protein sequence database derived from CHO-DG44 transcriptomic data was constructed to facilitate the identification of CHO-DG44 specific proteins. Using 2D RP/RPLC coupled to an LTQ Orbitrap XL mass spectrometer, we identified nearly 5,000 proteins and quantitated 2,800 with at least two peptides for downstream analysis. Although many previous articles studied a portion of cellular responses to high glucose environment, the findings in this article revealed crosstalk of these pathways through a systematic analysis. Pathway analysis revealed that in CHO cells cultured in high glucose media (15 g/L), oxidative phosphorylation and antioxidant response pathways were up-regulated when compared with the normal glucose media (5 g/L). Enhanced rDHFR expression was found in CHO cells in high glucose media, likely linked to the up-regulation of NCK1 and down-regulation of PRKRA. In addition, increased oxidative stress and recombinant protein expression affected biological functions in the mitochondria and ER, likely activating the mitochondria- and ER- mediated cell death pathways through the up-regulation of HtrA2 and calpains, respectively. Potential genetic engineering strategies for improved protein productivity and cell growth have been proposed. Specific productivity of recombinant proteins could potentially be enhanced by over-expression of NCK1 and knockdown of PRKRA, and cell death may be inhibited when knocking down HtrA2 and calpains (e.g., Capn1 and Capn5) in CHO cells.

Acknowledgment

This work was supported by NIH GM 15847 (to B.L.K.) and Alnylam Biotherapeutics. The authors thank Greg Thill for generating and providing CHO-DG44 cells expressing an empty vector that only contains DHFR gene. Contribution number 1031 from the Barnett Institute.

Nomenclature

2D = two dimensional
BP = biological process
Capn = calpain
CHO = Chinese hamster ovary
CID = collision-induced dissociation
DAVID = Database for Annotation, Visualization, and Integrated Discovery
DHFR = dihydrofolate reductase
ER = endoplasmic reticulum
FDR = false discovery rate
GO = gene ontology
HCD = higher-energy collisional dissociation
HTRA2 = high temperature requirement A 2
IPA = ingenuity pathway analysis
IVCD = integrated viable cell density
LC = liquid chromatography
LDH = lactate dehydrogenase
mAb = monoclonal antibody
MS = mass spectrometry
NCK1 = noncatalytic region of tyrosine kinase adaptor protein 1
PRKRA = protein kinase interferon-inducible double-stranded RNA-dependent activator
rDHFR = recombinant dihydrofolate reductase
ROS = reactive oxygen species
RP = reversed phase
SOM = self-organized map
TMT = tandem mass tag
UPR = unfolded protein response
VCD = viable cell density

Literature Cited

1. Walsh G. Biopharmaceutical benchmarks 2010. *Nat Biotechnol*. 2010; 28:917–924.
2. Kumar N, Gammell P, Clynes M. Proliferation control strategies to improve productivity and survival during CHO based production culture: a summary of recent methods employed and the effects of proliferation control in product secreting CHO cell lines. *Cytotechnology*. 2007; 53:33–46.

3. Griffin TJ, Seth G, Xie H, Bandhakavi S, Hu W-S. Advancing mammalian cell culture engineering using genome-scale technologies. *Trends Biotechnol*. 2007; 25:401–408.
4. Mazur X, Fussenegger M, Renner W, Bailey JE. Higher productivity of growth-arrested Chinese hamster ovary cells expressing the cyclin-dependent kinase inhibitor p27. *Biotechnol Prog*. 1998; 14:705–713.
5. Meleady P, Doolan P, Henry M, Barron N, Keenan J, O'Sullivan F, Clarke C, Gammell P, Melville M W, Leonard M, Clynes M. Sustained productivity in recombinant Chinese hamster ovary (CHO) cell lines: proteome analysis of the molecular basis for a process-related phenotype. *BMC Biotechnol*. 2011; 11:78.
6. Nissom PM, Sanny A, Kok YJ, Hiang YT, Chuah SH, Shing TK, Lee YY, Wong KTK, Hu W-S, Sim MYG, Philp R. Transcriptome and proteome profiling to understanding the biology of high productivity CHO cells. *Mol Biotechnol*. 2006; 34:125–140.
7. Palermo DP, DeGraaf ME, Marotti KR, Rehberg E, Post LE. Production of analytical quantities of recombinant proteins in Chinese hamster ovary cells using sodium butyrate to elevate gene expression. *J Biotechnol*. 1991; 19:35–47.
8. Rodriguez J, Spearman M, Huzel N, Butler M. Enhanced production of monomeric interferon-beta by CHO cells through the control of culture conditions. *Biotechnol Prog*. 2005; 21:22–30.
9. Kim TK, Ryu JS, Chung JY, Kim MS, Lee GM. Osmoprotective effect of glycine betaine on thrombopoietin production in hyperosmotic Chinese hamster ovary cell culture: clonal variations. *Biotechnol Prog*. 2000; 16:775–781.
10. Kaufmann H, Mazur X, Fussenegger M, Bailey JE. Influence of low temperature on productivity, proteome and protein phosphorylation of CHO cells. *Biotechnol Bioeng*. 1999; 63:573–582.
11. Wurm FM. Production of recombinant protein therapeutics in cultivated mammalian cells. *Nat Biotechnol*. 2004; 22:1393–1398.
12. Lim Y, Wong NSC, Lee YY, Ku SCY, Wong DCF, Yap MGS. Engineering mammalian cells in bioprocessing—current achievements and future perspectives. *Biotechnol Appl Biochem*. 2010; 55:175–189.
13. Chen K, Liu Q, Xie L, Sharp Pa, Wang DI. Engineering of a mammalian cell line for reduction of lactate formation and high monoclonal antibody production. *Biotechnol Bioeng*. 2001; 72: 55–61.
14. Ha H, Lee HB. Reactive oxygen species as glucose signaling molecules in mesangial cells cultured under high glucose. *Kidney Int*. 2000; 77:S19–S25.
15. Inoguchi T, Li P, Umeda F, Yu HY, Kakimoto M, Imamura M, Aoki T, Etoh T, Hashimoto T, Naruse M, Sano H, Utsumi H, Nawata H. High glucose level and free fatty acid stimulate protein kinase C-dependent activation of NAD(P)H oxidase in cultured vascular cells. *Diabetes*. 2000; 49:1939–1945.
16. Zhong Y, Li J, Chen Y, Wang JJ, Ratan R, Zhang SX. Activation of endoplasmic reticulum stress by hyperglycemia is essential for Müller cell-derived inflammatory cytokine production in diabetes. *Diabetes*. 2012; 61:492–504.
17. Harwood SM, Allen Da, Raftery MJ, Yaqoob MM. High glucose initiates calpain-induced necrosis before apoptosis in LLC-pk1 cells. *Kidney Int*. 2007; 71:655–663.
18. Fieder J, Schorn P, Bux R, Noé W. Increase of productivity in recombinant CHO-cells by enhanced glucose-levels. In: Beuvery EC, Griffiths JB, Zeijlemaker WP, editors. Animal Cell Technology: Developments Towards the 21st Century. The Netherlands: Springer; 1995:163–167.
19. Yuk IH, Zhang B, Yang Y, Dutina G, Leach KD, Vijayasankaran N, Shen AY, Andersen DC, Snedecor BR, Joly JC. Controlling glycation of recombinant antibody in fed-batch cell cultures. *Biotechnol Bioeng*. 2011; 108:2600–2610.
20. Baik JY, Lee GM. A DIGE approach for the assessment of differential expression of the CHO proteome under sodium butyrate addition: effect of Bcl-x(L) overexpression. *Biotechnol Bioeng*. 2010; 105:358–367.
21. Baik JY, Joo EJ, Kim YH, Lee GM. Limitations to the comparative proteomic analysis of thrombopoietin producing Chinese hamster ovary cells treated with sodium butyrate. *J Biotechnol*. 2008; 133:461–468.
22. Kantardjieff A, Jacob NM, Yee JC, Epstein E, Kok Y-J, Philp R, Betenbaugh M, Hu W-S. Transcriptome and proteome analysis of Chinese hamster ovary cells under low temperature and butyrate treatment. *J Biotechnol*. 2010; 145:143–159.
23. Carlage T, Hincapie M, Zang L, Lyubarskaya Y, Madden H, Mhatre R, Hancock WS. Proteomic profiling of a high-producing Chinese hamster ovary cell culture. *Anal Chem*. 2009; 81:7357–7362.
24. Carlage T, Hincapie M, Lyubarskaya Y, Weiskopf A, Hancock WS. Analysis of dynamic changes in the proteome of a Bcl-xl overexpressing Chinese hamster ovary cell culture during exponential and stationary phases. *Biotechnol Prog*. 2012; 28:814–823.
25. Yee JC. Genomic and proteomic exploration of CHO and hybridoma cells under sodium butyrate treatment. *Biotechnol Bioeng*. 2008; 99:1186–1204.
26. Lee MS, Kim KW, Kim YH, Lee GM. Proteome analysis of antibody-expressing CHO cells in response to hyperosmotic pressure. *Biotechnol Prog*. 2003; 19:1734–1741.
27. Baycin-Hizal D, Tabb DL, Chaerkady R, Chen L, Lewis NE, Nagarajan H, Sarkaria V, Kumar K, Wolozny D, Colao J, Jacobson E, Tian Y, O'Meally RN, Krag SS, Cole RN, Palsson BO, Zhang H, Betenbaugh M. Proteomic analysis of Chinese hamster ovary cells. *J Proteome Res*. 2012; 11:5265–5276.
28. Kang S, Ren D, Xiao G, Daris K, Buck L, Enyenihi A, Zubarev R, Bondarenko PV, Deshpande R. Cell line profiling to improve monoclonal antibody production. *Biotechnol Bioeng*. 2014; 111:748–760.
29. Farrell A, McLoughlin N, Milne JJ, Marison IW, Bones J. Application of multi-omics techniques for bioprocess design and optimization in Chinese hamster ovary cells. *J Proteome Res*. 2014; 13:3144–3159.
30. Xu X, Nagarajan H, Lewis NE, Pan S, Cai Z, Liu X, Chen W, Xie M, Wang W, Hammond S, Andersen MR, Neff N, Passarelli B, Koh W, Fan HC, Wang J, Gui Y, Lee KH, Betenbaugh MJ, Quake SR, Famili I, Palsson BO, Wang J. The genomic sequence of the Chinese hamster ovary (CHO)-k1 cell line. *Nat Biotechnol*. 2011; 29:735–741.
31. Lewis NE, Liu X, Li Y, Nagarajan H, Yerganian G, O'Brien E, Bordbar A, Roth A M, Rosenbloom J, Bian C, Xie M, Chen W, Li N, Baycin-Hizal D, Latif H, Forster J, Betenbaugh MJ, Famili I, Xu X, Wang J, Palsson BO. Genomic landscapes of Chinese hamster ovary cell lines as revealed by the *Cricetulus griseus* draft genome. *Nat Biotechnol*. 2013; 31:759–765.
32. Meleady P, Hoffrogge R, Henry M, Rupp O, Bort J H, Clarke C, Brinkrolf K, Kelly S, Müller B, Doolan P, Hackl M, Beckmann TF, Noll T, Grillari J, Barron N, Pühler A, Clynes M, Borth N. Utilization and evaluation of CHO-specific sequence databases for mass spectrometry based proteomics. *Biotechnol Bioeng*. 2012; 109:1386–1394.
33. Chinese Hamster Genome Database. Available at: http://www.chogenome.org.
34. Tummala S, Titus M, Wilson L, Wang C, Ciatto C, Thill G, Foster D, Li C, Szabo Z, Guttman A, Bettencourt B, Jayaraman M, Deroot J, Kocisko D, Pollard S, Charisse K, Kuchimanchi S, Hinkle G, Milstein S, Meyers R, Wu S-L, Karger BL, Rossomando A. Evaluation of exogenous siRNA addition as a metabolic engineering tool for modifying biopharmaceuticals. *Biotechnol Prog*. 2013; 29:415–424.
35. Gilar M, Olivova P, Daly AE, Gebler JC. Two-dimensional separation of peptides using RP-RP-HPLC system with different pH in first and second separation dimensions. *J Sep Sci*. 2005; 28:1694–1703.
36. Birzele F, Schaub J, Rust W, Clemens C, Baum P, Kaufmann H, Weith A, Schulz T W, Hildebrandt T. Into the unknown: expression profiling without genome sequence information in CHO by next generation sequencing. *Nucleic Acids Res*. 2010; 38:3999–4010.
37. Iseli C, Jongeneel C, Bucher P. ESTScan: a program for detecting, evaluating, and reconstructing potential coding regions in EST sequences. *Proc Int Conf Intell Syst Mol Biol*. 1999; 7: 138–148.

38. Dilly GF, Young CR, Lane WS, Pangilinan J, Girguis PR. Exploring the limit of metazoan thermal tolerance via comparative proteomics: thermally induced changes in protein abundance by two hydrothermal vent polychaetes. *Proc R Soc B*. 2012; 279:3347–3356.
39. Elias JE, Gygi SP. Target-decoy search strategy for increased confidence in large-scale protein identifications by mass spectrometry. *Nat Methods*. 2007; 4:207–214.
40. Gan CS, Chong PK, Pham TK, Wright PC. Technical, experimental, and biological variations in isobaric tags for relative and absolute quantitation (iTRAQ). *J Proteome Res*. 2007; 6:821–827.
41. Reich M, Liefeld T, Gould J, Lerner J, Tamayo P, Mesirov JP. GenePattern 2.0. *Nat Genet*. 2006; 38:500–501.
42. Kohonen T, Honkela T. Kohonen network. *Scholarpedia*. 2007; 2:1568.
43. Wolf-Yadlin A, Kumar N, Zhang Y, Hautaniemi S, Zaman M, Kim H-D, Grantcharova V, Lauffenburger D, White FM. Effects of her2 overexpression on cell signaling networks governing proliferation and migration. *Mol Syst Biol*. 2006; 2:54.
44. Tamayo P, Slonim D, Mesirov J, Zhu Q, Kitareewan S, Dmitrovsky E, Lander ES, Golub TR. Interpreting patterns of gene expression with self-organizing maps: methods and application to hematopoietic differentiation. *Proc Natl Acad Sci U S A*. 1999; 96:2907–2912.
45. Huang DW, Sherman BT, Tan Q, Kir J, Liu D, Bryant D, Guo Y, Stephens R, Baseler MW, Lane HC, Lempicki R. DAVID bioinformatics resources: expanded annotation database and novel algorithms to better extract biology from large gene lists. *Nucleic Acids Res*. 2007; 35:W169–W175.
46. Huang DW, Sherman BT, Lempicki R. Systematic and integrative analysis of large gene lists using DAVID bioinformatics resources. *Nat Protoc*. 2009; 4:44–57.
47. Gene T, Consortium O. Gene ontology: tool for the unification of biology. *Nat Genet*. 2000; 25:25–29.
48. Merico D, Isserlin R, Stueker O, Emili A, Bader GD. Enrichment map: a network-based method for gene-set enrichment visualization and interpretation. *PLoS One*. 2010; 5:e13984.
49. Shannon P, Markiel A, Ozier O, Baliga NS, Wang JT, Ramage D, Amin N, Schwikowski B, Ideker T. Cytoscape: a software environment for integrated models of biomolecular interaction networks. *Genome Res*. 2003; 13:2498–2504.
50. Urlaub G, Emmanuel K, Carothers AM, Chasin LA. Deletion of the diploid dihydrofolate reductase locus from cultured mammalian cells. *Cell*. 1983; 33:405–412.
51. Vishwanathan N, Le H, Jacob NM, Tsao YS, Ng S-W, Loo B, Liu Z, Kantardjieff A, Hu W-S. Transcriptome dynamics of transgene amplification in Chinese hamster ovary cells. *Biotechnol Bioeng*. 2014; 111:518–528.
52. Savitski MM, Sweetman G, Askenazi M, Marto J, Lang M, Zinn N, Bantscheff M. Delayed fragmentation and optimized isolation width settings for improvement of protein identification and accuracy of isobaric mass tag quantification on Orbitrap-type mass spectrometers. *Anal Chem*. 2011; 83:8959–8967.
53. Ting L, Rad R, Gygi SP, Haas W. Ms3 eliminates ratio distortion in isobaric multiplexed quantitative proteomics. *Nat Methods*. 2011; 8:937–940.
54. Moulder R, Lönnberg T, Elo LL, Filén J-J, Rainio E, Corthals G, Oresic M, Nyman T; Aittokallio T, Lahesmaa R. Quantitative proteomics analysis of the nuclear fraction of human CD4+ cells in the early phases of IL-4-induced Th2 differentiation. *Mol Cell Proteomics*. 2010; 9:1937–1953.
55. Salem M, Kenney PB, Rexroad CE, Yao J. Proteomic signature of muscle atrophy in rainbow trout. *J Proteomics*. 2010; 73: 778–789.
56. Dowling P, O'Driscoll L, O'Sullivan F, Dowd A, Henry M, Jeppesen PB, Meleady P, Clynes M. Proteomic screening of glucose-responsive and glucose non-responsive MIN-6 beta cells reveals differential expression of proteins involved in protein folding, secretion and oxidative stress. *Proteomics*. 2006; 6: 6578–6587.
57. Unwin RD, Smith DL, Blinco D, Wilson CL, Miller CJ, Evans C, Jaworska E, Baldwin S, Barnes K, Pierce A, Spooncer E, Whetton AD. Quantitative proteomics reveals posttranslational control as a regulatory factor in primary hematopoietic stem cells. *Blood*. 2006; 107:4687–4694.
58. Wang J, Jiang J, Zhang H, Wang J, Cai H, Li C, Li K, Liu J, Guo X, Zou G, Wang D, Deng Y, Dai J. Integrated transcriptional and proteomic analysis with in vitro biochemical assay reveal the important role of CYP3A46 in T-2 toxin hydroxylation in porcine primary hepatocytes. *Mol Cell Proteomics*. 2011; 10:008748.
59. Hao J, Zhu L, Zhao S, Liu S, Liu Q, Duan H. PTEN ameliorates high glucose-induced lipid deposits through regulating SREBP-1/FASN/ACC pathway in renal proximal tubular cells. *Exp Cell Res*. 2011; 317:1629–1639.
60. Kaplan M, Kerry R, Aviram M, Hayek T. High glucose concentration increases macrophage cholesterol biosynthesis in diabetes through activation of the sterol regulatory element binding protein 1 (srebp1): inhibitory effect of insulin. *J Cardiovasc Pharmacol*. 2008; 52:324–332.
61. Chen Y-H, Chen J-Y, Chen Y-W, Lin S-T, Chan H-L. High glucose-induced proteome alterations in retinal pigmented epithelium cells and its possible relevance to diabetic retinopathy. *Mol BioSyst*. 2012; 8:3107–3124.
62. Russell JW, Golovoy D, Vincent AM, Mahendru P, Olzmann J, Mentzer A, Feldman E. High glucose-induced oxidative stress and mitochondrial dysfunction in neurons. *FASEB J*. 2002; 16: 1738–1748.
63. Fagone P, Jackowski S. Membrane phospholipid synthesis and endoplasmic reticulum function. *J Lipid Res*. 2009; 50(Suppl): S311–S316.
64. Thakur A, Bollig A, Wu J, Liao DJ. Gene expression profiles in primary pancreatic tumors and metastatic lesions of Ela-c-myc transgenic mice. *Mol Cancer*. 2008; 7:11.
65. Donati G, Montanaro L, Derenzini M. Ribosome biogenesis and control of cell proliferation: p53 is not alone. *Cancer Res*. 2012; 72:1602–1607.
66. Huang C, Kim Y, Caramori ML, Moore JH, Rich SS, Mychaleckyj JC, Walker PC, Mauer M. Diabetic nephropathy is associated with gene expression levels of oxidative phosphorylation and related pathways. *Diabetes*. 2006; 55:1826–1831.
67. Waanders LF, Chwalek K, Monetti M, Kumar C, Lammert E, Mann M. Quantitative proteomic analysis of single pancreatic islets. *Proc Natl Acad Sci U S A*. 2009; 106:18902–18907.
68. Morrison J, Knoll K, Hessner MJ, Liang M. Effect of high glucose on gene expression in mesangial cells: upregulation of the thiol pathway is an adaptational response. *Physiol Genomics*. 2004; 17:271–282.
69. Xu C, Bailly-Maitre B, Reed JC. Endoplasmic reticulum stress: cell life and death decisions. *J Clin Invest*. 2005; 115:2656–2664.
70. Walter P, Ron D. The unfolded protein response: from stress pathway to homeostatic regulation. *Science*. 2011; 334:1081–1086.
71. Wurm FM, Hacker D. First CHO genome. *Nat Biotechnol*. 2011; 29:718–720.
72. Latreille M, Larose L. Nck in a complex containing the catalytic subunit of protein phosphatase 1 regulates eukaryotic initiation factor 2alpha signaling and cell survival to endoplasmic reticulum stress. *J Biol Chem*. 2006; 281:26633–26644.
73. Kebache S, Cardin E, Nguyên DT, Chevet E, Larose L. Nck-1 antagonizes the endoplasmic reticulum stress-induced inhibition of translation. *J Biol Chem*. 2004; 279:9662–9671.
74. Peters GA, Hartmann R, Qin JUN. Modular structure of PACT: distinct domains for binding and activating PKR. *Mol Cell Biol*. 2001; 21:1908–1920.
75. Dinnis DM, James DC. Engineering mammalian cell factories for improved recombinant monoclonal antibody production: lessons from nature? *Biotechnol Bioeng*. 2005; 91:180–189.
76. Liu Q-B, Liu L-L, Lu Y-M, Tao R-R, Huang J-Y, Shioda N, Moriguchi S, Fukunaga K, Han F, Lou Y-J. The induction of reactive oxygen species and loss of mitochondrial omi/HtrA2 is associated with *S*-nitrosoglutathione-induced apoptosis in human endothelial cells. *Toxicol Appl Pharmacol*. 2010; 244:374–384.
77. Martins LM, Iaccarino I, Tenev T, Gschmeissner S, Totty NF, Lemoine NR, Savopoulos J, Gray CW, Creasy CL, Dingwall C, Downward J. The serine protease omi/HtrA2 regulates apoptosis

by binding XIAP through a reaper-like motif. *J Biol Chem*. 2002; 277:439–444.

78. Hegde R, Srinivasula SM, Zhang Z, Wassell R, Mukattash R, Cilenti L, DuBois G, Lazebnik Y, Zervos AS, Fernandes-Alnemri T, Alnemri ES. Identification of omi/HtrA2 as a mitochondrial apoptotic serine protease that disrupts inhibitor of apoptosis protein-caspase interaction. *J Biol Chem*. 2002; 277: 432–438.
79. Jesenberger V, Jentsch S. Deadly encounter: ubiquitin meets apoptosis. *Nat Rev Mol Cell Biol*. 2002; 3:112–121.
80. Ma H, Yang HQ, Takano E, Lee WJ, Hatanaka M, Maki M. Requirement of different subdomains of calpastatin for calpain inhibition and for binding to calmodulin-like domains. *J Biochem*. 1993; 113:591–599.
81. Weber H, Hühns S, Lüthen F, Jonas L, Schuff-Werner P. Calpain activation contributes to oxidative stress-induced pancreatic acinar cell injury. *Biochem Pharmacol*. 2005; 70:1241–1252.
82. Nakagawa T, Yuan J. Cross-talk between two cysteine protease families. Activation of caspase-12 by calpain in apoptosis. *J Cell Biol*. 2000; 150:887–894.
83. Syntichaki P, Xu K, Driscoll M, Tavernarakis N. Specific aspartyl and calpain proteases are required for neurodegeneration in *C. elegans*. *Nature*. 2002; 419:939–944.
84. Wong DCF, Wong KTK, Nissom PM, Heng CK, Yap GMS. Targeting early apoptotic genes in batch and fed-batch CHO cell cultures. *Biotechnol Bioeng*. 2006; 95:350–361.

Manuscript received Jul. 29, 2014, and revision received Mar. 11, 2015.